Neurochemistry International 190 (2025) 106048

Contents lists available at ScienceDirect

Neurochemistry International

journal homepage: www.elsevier.com/locate/neuint

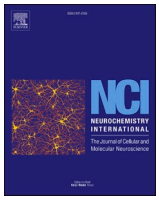

# Impaired lysosomal proteolysis in developing neurons induces protein aggregation and disrupts morphogenesis and neuromaturation

Yinping Zhou [a,1], Yuuki Fujiwara [a,1,*], Mai Shirazaki [b,c], Xiaoye Tian [a], Gen Igarashi [d], Hiroto Yamauchi [e], Kazunori Imaizumi [a,f], Hideki Hayakawa [a], Ko Miyoshi [a], Taiichi Katayama [a]

[a] Department of Child Development and Molecular Brain Science, United Graduate School of Child Development, Osaka University, Suita, Osaka, 565-0871, Japan
[b] Nikon Imaging Center, Osaka University, Suita, Osaka, 565-0871, Japan
[c] Department of Immunology and Cell Biology, Graduate School of Medicine and Frontier Biosciences, Osaka University, Suita, Osaka, 565-0871, Japan
[d] Faculty of Medicine, Osaka University, Suita, Osaka, 565-0871, Japan
[e] Division of Medicine, Graduate School of Medicine, Osaka University, Suita, Osaka, 565-0871, Japan
[f] The Osaka Medical Research Foundation for Intractable Diseases, Osaka, 558-0041, Japan

ARTICLE INFO

*Keywords:*
Lysosome
Proteolysis
Protein aggregation
Proteostasis
Neuromaturation
Neurodevelopment

ABSTRACT

Lysosomes play a central role in the degradation of intracellular substances. Through this degradative capacity, lysosomes contribute to biological homeostasis and are particularly critical for the maintenance and function of neurons. Deficiencies in various lysosomal proteins cause a group of conditions known as lysosomal storage disorders, which often present with developmental delay and other neurological symptoms. In addition, defects in lysosomal function and the autophagic pathways that deliver intracellular substrates to lysosomes have been linked to neurodevelopmental disorders. However, the contribution of lysosomal degradative capacity to neurodevelopment has not been well appreciated. In this study, we aimed to examine the relationship between overall lysosomal proteolytic capacity and neuronal development using primary cultured neurons at early developmental stages. We found that lysosomal protein expression and proteolytic activity increased with neuronal maturation, suggesting that lysosomal proteolysis may play an important role in neuronal development. Treatment of cultured neurons with specific inhibitors of lysosomal proteases during development impaired morphogenesis, as indicated by a significant decrease in neurite length and complexity, along with decreased expression of neuronal lineage marker proteins. Furthermore, we observed that neurons with development impaired by lysosomal protease inhibition accumulated aggregated proteins—some of which were ubiquitinated—in the cytoplasm. These aggregates were enriched with various proteins related to neurodevelopment. These findings provide new insights into the previously underappreciated role of lysosomes in neuronal development.

## 1. Introduction

Lysosomes are the primary sites for the degradation of virtually all types of macromolecules in cells (de Duve et al., 1955). They play pivotal roles in biological homeostasis and are particularly critical for the maintenance and function of neurons (Ballabio and Bonifacino, 2020). Multiple intracellular pathways that deliver cytoplasmic substances into lysosomes are collectively known as autophagy (Yim and Mizushima, 2020). Lysosomal dysfunction in neurons impairs intracellular degradation capacity, leading to protein accumulation and neurotoxicity. One group of diseases caused by lysosomal dysfunction is known as lysosomal storage disorders (LSDs). Studies on LSDs have reported neuronal symptoms including developmental defects, suggesting a potential role for lysosomes in neurodevelopment (Ballabio and Bonifacino, 2020; Platt et al., 2018). Additionally, lysosomal dysfunction has been implicated in the pathogenesis of late-onset neurodegenerative diseases such as Alzheimer's disease and Parkinson's disease (Nixon and Rubinsztein, 2024). Interestingly, the accumulation of α-synuclein protein aggregates—originally known as a hallmark of late-onset neurodegenerative diseases such as Parkinson's disease and

* Corresponding author. Department of Child Development and Molecular Brain Science, United Graduate School of Child Development, Osaka University, 2-2 Yamadaoka, Suita, Osaka, 565-0871, Japan.
*E-mail address:* yuuki.fujiwara@ugscd.osaka-u.ac.jp (Y. Fujiwara).
[1] These authors contributed equally to this work.

https://doi.org/10.1016/j.neuint.2025.106048
Received 3 June 2025; Received in revised form 14 August 2025; Accepted 29 August 2025
Available online 30 August 2025

dementia with Lewy bodies—is also evident in patients with multiple LSDs and their animal models (Navarro-Romero et al., 2020). This suggests that LSDs and geriatric neurodegenerative diseases may share a certain overlap in their pathomechanisms, as both are associated with the accumulation of aggregated proteins in neurons.

During neurodevelopment, the maintenance of intracellular homeostasis is critical. Many previous studies have shown that disruptions in synthetic systems can lead to deficiencies in neural factors, thereby contributing to neurodevelopmental disorders (Lo and Lai, 2020). In contrast, studies on the role of degradation systems in neurodevelopment remain limited. The mammalian/mechanistic target of rapamycin (mTOR), a master regulator of cellular metabolism and growth, regulates autophagy, lysosome biogenesis, and other biological processes by participating in multiple intracellular signaling pathways (Battaglioni et al., 2022). Genetic studies have identified an association between dysregulated mTOR signaling and neurodevelopmental disorders (Parenti et al., 2020). This dysregulation suggests that abnormal autophagic and lysosomal processes may impair neurodevelopment. Furthermore, recent studies have highlighted the role of macroautophagy, the most extensively studied pathway in autophagy, in neurodevelopment and its possible disruption in the pathogenesis of neurodevelopmental disorders (Collier et al., 2021; Hui et al., 2019; Linda et al., 2022). However, most such studies focus primarily on the relationship between neurodevelopment and a single autophagic pathway, macroautophagy. Notably, the accumulation of aggregated proteins has been reported as a potential pathogenic mechanism in neurodevelopmental disorders, based on a study using mice with macroautophagy deficiency specifically in mature adolescent neurons that exhibit autism spectrum disorder (ASD)-like phenotypes (Hui et al., 2019). These findings suggest that the insufficiency in degradative function of lysosomes and the resulting accumulation of aggregated proteins may contribute to the pathogenesis of neurodevelopmental disorders, as well as LSDs and neurodegenerative disorders. However, the independent role of lysosomes, particularly their degradative capacity, in neurodevelopment requires further investigation.

In this study, we focused on the relationship between lysosomal degradative capacity and neurodevelopment processes. Primary cultured hippocampal neurons are well-established models for studying neuronal development (Banker, 2018). In culture, rat hippocampal neurons initially develop multiple morphologically identical neurites. After 2 days *in vitro* (DIV), most neurons acquire polarity, forming a single long neurite that eventually becomes an axon and several shorter neurites that mature into dendrites. Within approximately 1 week of culture, these neurites differentiate into a distinct axon and multiple dendrites (Banker, 2018; Dotti et al., 1988).

In this study, we aimed to examine the effect of impaired overall lysosomal proteolytic capacity on developing primary cultured neurons in an early stage of maturation. As lysosomes contain approximately 60 hydrolases, including more than 10 proteases (Appelqvist et al., 2013), it is difficult to selectively disrupt their proteolytic function through genetic approaches without affecting other components. Therefore, we took advantage of pepstatin A and E64d, which are specific inhibitors of lysosomal proteases with minimal side effects and low toxicity (Tanida et al., 2005).

## 2. Materials and methods

### 2.1. Primary culture of rat hippocampal neurons

Hippocampi were dissected from embryonic day 18–18.5 (E18–18.5) Wistar rat brains and dissociated using 0.66 μg/mL papain (Worthington Biochemical Corp., LS003119) in phosphate-buffered saline (PBS) containing 0.18 % glucose (Sigma, G7528), 0.1 % bovine serum albumin (Sigma, A7906), and 12 μg/mL of DNase I (Sigma, DN25) for 20 min at 37 °C. The papain-containing solution was then replaced with the same buffer lacking papain by serial pipetting using a Pasteur pipette. After each round of pipetting, the solution containing dissociated neurons was collected, and fresh buffer was added for the next round. The dissociated neurons were collected by centrifugation, resuspended in Neurobasal Medium (Gibco, 21103049) supplemented with 10 % Fetal Clone III (HyClone, SH30109.03), and seeded onto culture plates, glass coverslips, or chambers pre-coated with poly-D-lysine (Sigma, P6407). Following 4 h of incubation, the medium was replaced with Neurobasal medium supplemented with 2 % B-27 (Gibco, 17504044) and 1 % GlutaMAX (Gibco, 35050061). Thereafter, half of the medium was replaced with fresh medium every 3 days. For immunoblotting assays, $5.0 \times 10^5$ cells/well, $2.0 \times 10^5$ cells/well, or $5.0 \times 10^5$ cells/dish of neurons were seeded in 6-well plates (Thermo Scientific, 140675), 12-well plates (Thermo Scientific, 150628), or 35-mm dishes (Iwaki, 3000-035-MYP), respectively. For quantitative RT-PCR, $5.0 \times 10^4$ cells/well of neurons were seeded in 24-well plates (Thermo Scientific, 142475). For pulse-chase assays, $2.0 \times 10^5$ cells/well of neurons were seeded in 24-well plates. For fluorescence imaging in Fig. 1g and h, $3.0 \times 10^4$ cells/dish of neurons were seeded in 35-mm glass base dishes (Iwaki, 3961-035). For fluorescence imaging in Fig. 3a–f and k, neurons were seeded on micro cover glass (Matsunami, C013001) immersed in 24-well plates at a density of $2.0 \times 10^5$ cells/well; for Fig. 3g–j, a density of $2.5 \times 10^4$ cells/well was used. For fluorescence imaging in Supplementary Fig. 1b–c, 2a, and 3a, $6.0 \times 10^4$ cells/well, $3.0 \times 10^4$ cells/well, and $1.2 \times 10^5$ cells/well of neurons were seeded in 4-chamber slides, respectively (Falcon, 354114). For the lactate dehydrogenase (LDH) assay, $1.0 \times 10^5$ cells/well of neurons were seeded in 24-well plates. In experiments using pepstatin A and E64d, the culture medium was supplemented from DIV 1 with either 1:2500 volume of dimethyl sulfoxide (DMSO, control) or 10 μg/mL of pepstatin A (Peptide Institute, 4397) and E64d (Peptide Institute, 4321-v) in the same volume of DMSO. For the measurement of cytotoxicity, LDH assay was performed using LDH Cytotoxicity Assay Kit (Nacalai Tesque, 18250-64) according to the manufacturer's instructions. In experiments using ammonium chloride, the culture medium was supplemented from DIV 1 with 20 mM ammonium chloride. All animal experiments were conducted in strict accordance with the guidelines of Osaka University and were approved by the Animal Experiments Committee of Osaka University.

### 2.2. Immunoblotting

Primary cultured hippocampal neurons prepared for each assay were solubilized in sodium dodecyl sulphate-polyacrylamide gel electrophoresis (SDS-PAGE) sample buffer (10 mM Tris-HCl [pH 7.8], 3 % SDS, 5 % glycerol, 0.02 % bromophenol blue, and 2 % 2-mercaptoethanol) and subjected to SDS-PAGE. Following electrophoretic separation (ATTO, E-R520L), the proteins were transferred onto polyvinylidene difluoride membranes (Millipore, IPVH00010). Membranes were blocked with 3 % bovine serum albumin and 0.01 % sodium azide in PBS, then incubated overnight at 4 °C with primary antibodies diluted in the same blocking buffer. The next day, membranes were washed with PBS containing 0.1 % Tween 20 and incubated with secondary antibodies diluted in the same wash buffer for 1 h at room temperature. The membranes were then treated with ECL Start Western Blotting Detection Reagent (Amersham, RPN3243) or ECL Prime Western Blotting Detection Reagent (Amersham, RPN2236), and signal bands were visualized using PX Fuji Medical X-RAY Film (Fujifilm, 47410 07544) and CEPROS Q (Fujifilm). The following antibodies were used for immunoblotting: rabbit polyclonal anti-lysosome-associated membrane protein 1 (LAMP1) antibody (Bioss Antibodies, bs-1970R), rabbit monoclonal anti-lysosomal integral membrane protein II (LIMPII) antibody (EPR12080, abcam, ab176317), mouse monoclonal anti-cathepsin D antibody (Proteintech, 66534-1-Ig), rabbit monoclonal anti-transcription factor EB (TFEB) antibody (E5P9M, Cell Signaling Technology, 83010), rabbit monoclonal anti-phospho-TFEB (Ser122) antibody (E9M5M, Cell Signaling Technology, 87932), rabbit monoclonal anti-phospho-S6 ribosomal protein (Ser240/244) antibody (D68F8,

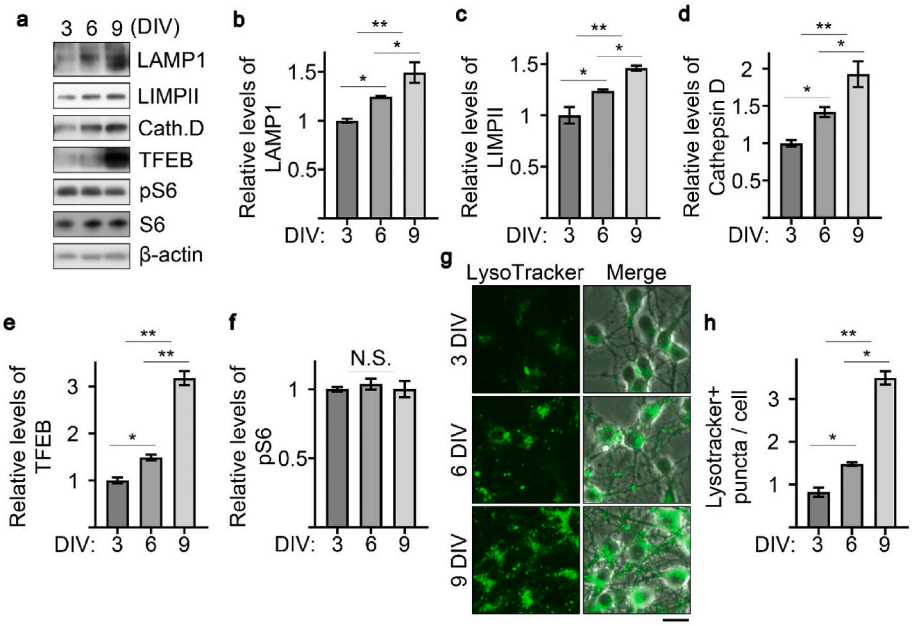


**Fig. 1.** Expression levels of lysosomal proteins in cultured neurons during neuromaturation (a) Immunoblotting of lysosomal proteins and other related proteins in primary cultured hippocampal neurons in 3, 6, and 9 days *in vitro* (DIV). (b–f) Quantification of the relative levels of LAMP1 (b), LIMPII (c), Cathepsin D (d), TFEB (e) and phosphorylated S6 ribosomal protein (f) in primary cultured hippocampal neurons in each DIV. (n = 3–5). (g) Fluorescence microscopy images of primary cultured neurons in 3, 6, and 9 DIV, labeled with LysoTracker. (h) Quantification of the number of Lysotracker-positive puncta per neurons. (n = 41–85 cells). Bar represents 20 μm $*p < 0.05$, $**p < 0.01$; N.S., not significant.

Cell Signaling Technology, 5364), rabbit monoclonal anti-S6 ribosomal protein antibody (5G10, Cell Signaling Technology, 2217), mouse monoclonal anti-β-actin antibody (AC-15, Sigma-Aldrich, A1978), mouse monoclonal anti-multiubiquitin chain antibody (FK2, Cayman Chemical, 14220), rabbit monoclonal anti-β3-tubulin antibody (D71G9, Cell Signaling Technology, 5568), rabbit monoclonal anti-NeuN (Fox-3) antibody (D4G4O, Cell Signaling Technology, 24307), rabbit polyclonal anti-microtubule-associated protein 2 (MAP2) antibody (Cell Signaling Technology, 4542), horseradish peroxidase (HRP)-linked anti-rabbit immunoglobulin G (IgG) antibody (Cell Signaling Technology, 7074), and HRP-linked anti-mouse IgG antibody (Cell Signaling Technology, 7076).

### 2.3. Quantitative RT-PCR

Primary cultured hippocampal neurons were eluted in TRI Reagent (MRC, TR118) and total RNA was purified according to the manufacturer's instructions. The cDNA was then synthesized using the Quanti-Tech Reverse Transcription Kit (QIAGEN, 205313), and subjected to real-time quantitative PCR using SYBR Premix Ex *Taq*II (Tli RNaseH Plus) (TaKaRa) and LightCycler 96 System (Roche, 05815916001). The expression levels of TFEB were quantified in relation to GAPDH. The following primers were used: Rat GAPDH: 5′- GCTGA-GAATGGGAAGCTGGT -3′ and 5′- ACGACATACTCAGCACCAGC -3′, and rat TFEB: 5′- CGACAACATTATGCGCCTGG -3′ and 5′- CTGTA-CACGTTCAGGTGGCT -3′. The primer sequences were generated using Primer3Plus (http://www.bioinformatics.nl/cgi-bin/primer3plus/primer3plus.cgi/) and specificity was confirmed by BLAST searches.

### 2.4. Fluorescence microscopy

Primary cultured hippocampal neurons were incubated at 37 °C for 30 min at 3, 6, or 9 DIV with LysoTracker™ Green DND-26 (Invitrogen, L7526) at a 1:1000 dilution. Following incubation, cells were washed with Neurobasal Medium supplemented with 2 % B-27 and 1 % Gluta-MAX, then replaced with the same medium. Fluorescence imaging was performed using an FV10i-LIV confocal microscope (Olympus) (Fig. 1e and f), and the number of LysoTracker + puncta/cell was quantified by dividing the total number of LysoTracker + puncta in each image by the number of cell bodies (DAPI).

Primary hippocampal neurons were cultured on glass coverslips or 4-chamber slides for each assay until 3, 6, or 9 DIV. Neurons were then fixed with 4 % paraformaldehyde in phosphate buffer (Nacalai Tesque, 09154-85) for 30 min on ice, washed twice with PBS, and blocked/permeabilized with PBS containing 10 % goat serum (Gibco, 16210064) and 0.5 % Triton X-100 for 1 h at room temperature. Cells were incubated overnight at 4 °C with either rabbit monoclonal anti-TFEB antibody or mouse monoclonal anti-Tau1 antibody (PC1C6, Chemicon, MAB3420) diluted in the same blocking buffer. The following day, cells were washed twice with PBS and incubated with a fluorescently labeled secondary antibody (A-11011 or A-11004, Invitrogen) for 1 h at room temperature. Imaging was performed using AX R ECLIPSE Ti2-E confocal microscope (Nikon) or ECLIPSE Ti confocal microscope (Nikon) (Fig. 3g–j, Supplementary Fig. 1b and 2a).

Primary hippocampal neurons cultured on glass coverslips were maintained in the presence or absence of pepstatin A and E64d and transfected at 5 DIV with 0.5 μg/well of a pCI-neo vector expressing enhanced green fluorescent protein (EGFP), using Lipofectamine™ 3000 reagent (Invitrogen). The following day, neurons were fixed with 4 % paraformaldehyde in phosphate buffer for 30 min on ice, washed twice with PBS, and stained using the Proteostat® Aggresome Detection Kit (Enzo, ENZ-51035), according to the manufacturer's instructions. The cells were then mounted with VECTASHIELD® HardSet™ Antifade Mounting Medium with DAPI (Vector Laboratories, H-1500), and confocal imaging was performed using an AX R ECLIPSE Ti2-E confocal microscope (Fig. 3a–f and k).

Primary hippocampal neurons cultured on 4-chamber slides were maintained in the presence or absence of ammonium chloride and transfected at 5 DIV with 0.3 μg/well of a pCI-neo vector expressing EGFP, using Lipofectamine™ 3000 reagent. During the transfection, the medium was replaced with fresh medium without ammonium chloride for 6 h. The following day, neurons were fixed with 4 %

paraformaldehyde in phosphate buffer for 30 min on ice, washed twice with PBS, and mounted with VECTASHIELD® HardSet™ Antifade Mounting Medium with DAPI, then confocal imaging was performed using an AX R ECLIPSE Ti2-E confocal microscope (Supplementary Fig. 3a).

### 2.5. Pulse-chase assay

Primary cultured hippocampal neurons were radiolabeled with tritium-labeled leucine by adding 37 kBq/well of leucine L-[4,5-$^3$H(N)]- (PerkinElmer, NET1166001MC) to the medium for 2 days starting from 1 DIV. At 3 DIV, the medium was replaced with fresh medium containing 8 mM non-labeled leucine, following a wash with the same non-radioactive medium. Neurons designated for collection at 3 DIV were collected immediately after washing using 500 μL/well of trypsin (Gibco, 25200-056). Neurons collected at 6 and 9 DIV were cultured in the presence or absence of pepstatin A and E64d until the indicated timepoints and then collected using the same procedure. Thereafter, the trypsinized cells (500 μL/well) were mixed with an equal volume of 10 % trichloroacetic acid (TCA) and placed on ice for 10 min, followed by centrifugation at 6500×*g* for 10 min at 4 °C. The resulting TCA-insoluble pellet, containing intact proteins, was resuspended in 0.1 % SDS in 2 M NaOH. The solubilized samples were mixed with Ultima Gold scintillation cocktail (PerkinElmer, 6013321), and the radioactivity was measured using an AccuFLEX LSC-7400 liquid scintillation counter (ALOKA) (Fig. 2a).

Primary cultured hippocampal neurons were radiolabeled with the same tritium-labeled leucine for 2 days, starting from 1 or 7 DIV. Radiolabeled intact proteins were then collected at 0 and 3 days post-labeling using the same procedure as described above. Relative protein degradation levels were assessed by subtracting the radioactivity in samples collected 0 days post-labeling from that in day 3 samples. Lysosomal protein degradation was assessed by subtracting the total degradation levels in pepstatin A- and E64d-treated neurons from those in untreated (control) neurons (Fig. 2b–e).

### 2.6. Pull-down assay and mass spectrometry analysis

To prepare the Triton X-100-soluble and -insoluble fractions, primary cultured rat hippocampal neurons (6 DIV) cultured in the presence or absence of pepstatin A and E64d were solubilized in 1 % Triton X-100 lysis buffer (50 mM Tris-HCl [pH 7.5], 150 mM NaCl, 5 mM EDTA, and 1 % Triton X-100) supplemented with cOmplete™ EDTA-free (Roche, 04693132001), PhosSTOP™ (Roche, 04906845001), and 50 μM PR-619 (LifeSensors, SI9619). The lysates were rotated at 4 °C for 15 min, followed by centrifugation at 17,700×*g* for 10 min at 4 °C. The supernatants were collected as the Triton X-100-soluble fraction, and after protein concentration normalization, were mixed with 3 × SDS-PAGE sample buffer. The resulting Triton X-100-insoluble pellets were resuspended in RIPA buffer without SDS (Nacalai Tesque, 08714-04), supplemented as above, and solubilized by sonication using a Handy Sonic (TOMY, UR-20P). The samples were again centrifuged at 17,700×*g* for 10 min at 4 °C, and the supernatants were collected as the Triton X-100-insoluble fraction. The concentrations of the insoluble fractions were normalized using the same dilution factor as for the soluble fractions. A portion of each sample was mixed directly with 3 × SDS-PAGE sample buffer, while the remainder was used for the pull-down assay. For pull-down assay, the Triton X-100-insoluble fraction were incubated with ~50 μL/sample of either control agarose (LifeSensors, UM400) or Agarose-TUBE2 beads (LifeSensors, UM402) and rotated at 4 °C for 4 h. The beads were then washed three times with RIPA buffer without SDS (containing the same inhibitors), and bound proteins were eluted in SDS-PAGE sample buffer. The eluates were subjected to immunoblotting, silver staining, and mass spectrometry analysis. For mass spectrometry, gel-based shotgun proteomic analyses were conducted by LC-MS/MS following silver staining of the proteins pulled down with

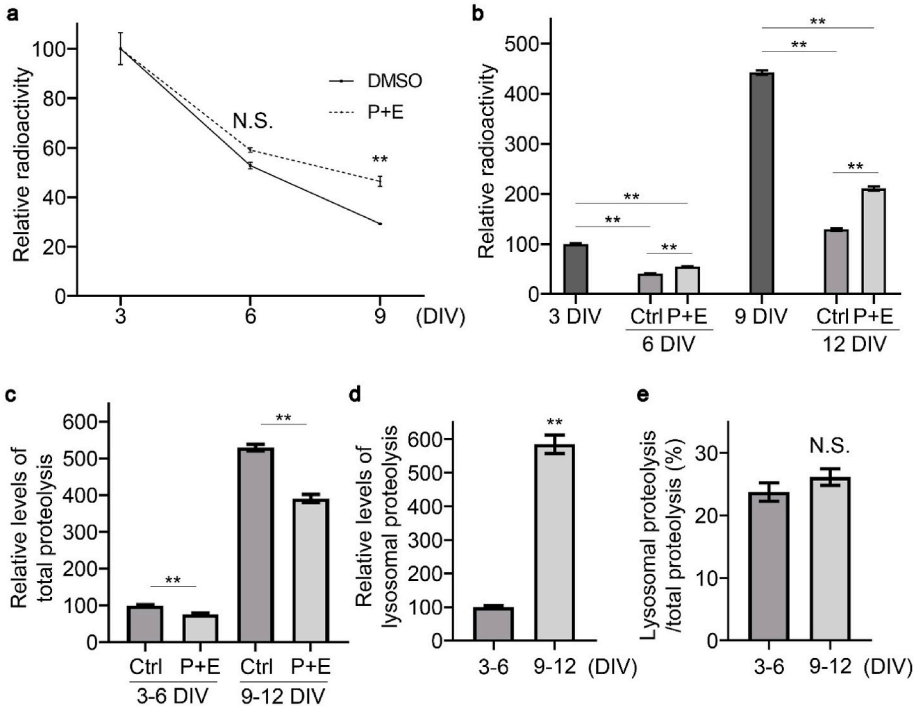


**Fig. 2.** Degradation levels of proteins in cultured neurons under lysosomal protease inhibition during neuromaturation (a) Levels of radiolabeled total protein in primary cultured hippocampal neurons cultured in the presence or absence of pepstatin A and E64d from 3 DIV to indicated time points. (b) Levels of radiolabeled total protein in primary cultured hippocampal neurons cultured in the presence or absence of pepstatin A and E64d from 3 or 9 DIV to 6 or 12 DIV, respectively. (c) Relative levels of total protein degradation in control and pepstatin A- and E64d-treated neurons during 3–6 DIV and 9–12 DIV. (d) Relative levels of lysosomal proteolysis in neurons during 3–6 and 9–12 DIV. (e) Percentage of lysosomal proteolysis levels to total protein degradation levels in neurons during 3–6 and 9–12 DIV. (n = 4). *$p < 0.05$, **$p < 0.01$; N.S., not significant. P + E, pepstatin A and E64d.

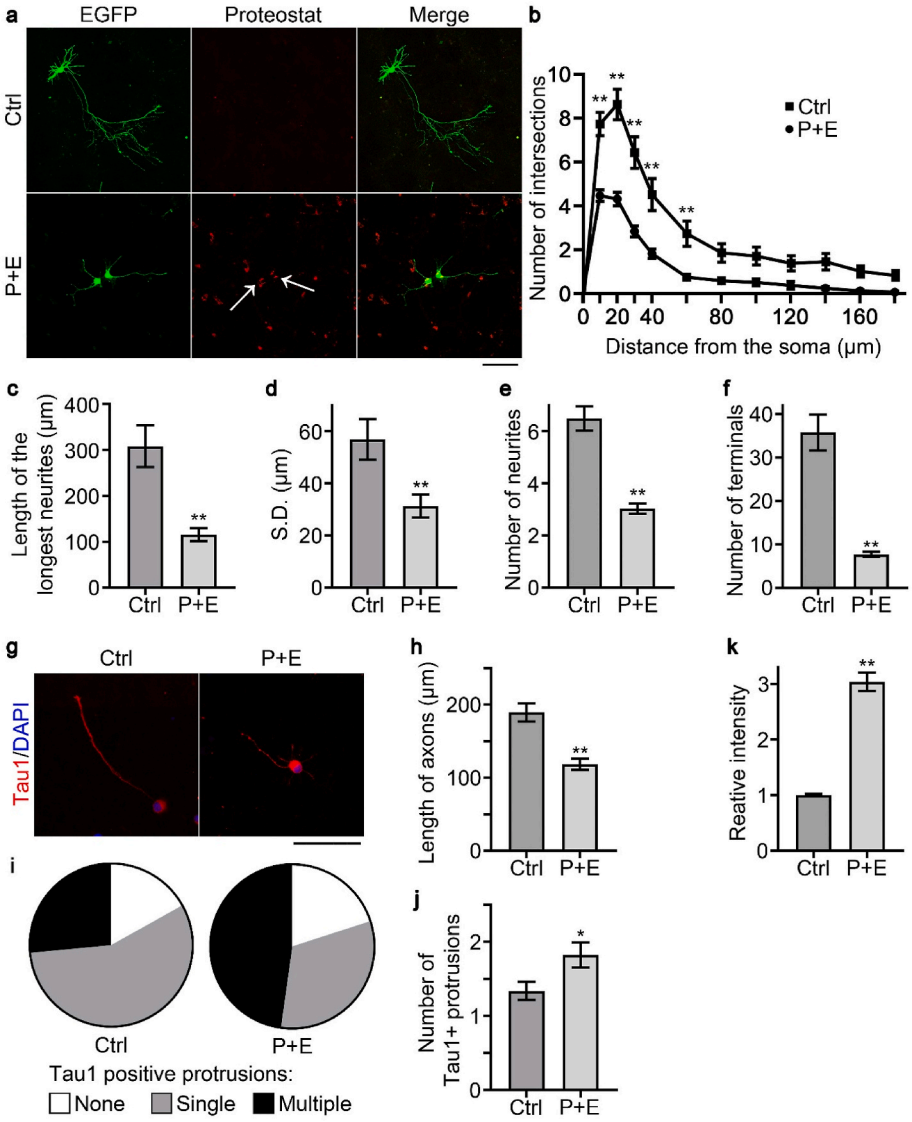


**Fig. 3.** Morphological features and accumulation of aggregated proteins in cultured neurons under lysosomal proteolysis inhibition during neuromaturation (a) Representative image of primary cultured hippocampal neurons cultured in the presence or absence of pepstatin A and E64d (6 DIV). Arrows indicate Proteostat signals in the EGFP-expressing neurons. Statistical analyses for the same neurons are presented in B–F and K. (b–f) Sholl analyses of neurites (Ctrl: n = 67, P + E: n = 67) (b), length of the longest neurite in each cell (Ctrl: n = 46, P + E: n = 69) (c), standard deviation of the difference in length between the longest neurites and other neurites in the same neurons (Ctrl: n = 46, P + E: n = 69) (d), number of neurites (Ctrl: n = 46, P + E: n = 69) (e), and neurite terminals per cell (Ctrl: n = 46, P + E: n = 69) (f) in neurons cultured in the presence or absence of pepstatin A and E64d (6 DIV). (g) Representative image of primary cultured hippocampal neurons cultured in the presence or absence of pepstatin A and E64d (3 DIV), immunostained with anti-Tau1 antibody. Statistical analyses for the same neurons are presented in h–j. (h–j) Length of axons (Ctrl: n = 31, P + E: n = 47) (h), Distribution of neurons with no, single, or multiple Tau1-positive protrusions (Ctrl: n = 31, P + E: n = 47) (i), and number of Tau1-positive protrusions (Ctrl: n = 83, P + E: n = 91) (j) in neurons cultured in the presence or absence of pepstatin A and E64d (3 DIV). An axon was defined as the longest Tau1-positive neurite among the neurons with multiple Tau1-positive protrusions. (k) Quantification of the relative levels of Proteostat-positive signals in neurons cultured in the presence or absence of pepstatin A and E64d (6 DIV) (Ctrl: n = 113, P + E: n = 113). Bars represent 100 μm*$p <$ 0.05, **$p < 0.01$; N.S., not significant. P + E, pepstatin A and E64d.

Agarose-TUBE2 beads, using a glutaraldehyde-free silver staining kit (Apro Science, SP-4020). The mass spectrometry was performed as a custom service by the Center of Medical Innovation and Translational Research (CoMIT) Omics Center, Osaka University. The resulting data were processed using Mascot Distiller v2.8 (Matrix Science) and analyzed with Scaffold 5 (Proteome Software).

### 2.7. Statistical analyses

Tukey's test and Student's *t*-test were used for comparisons among more than two groups and between two groups, respectively. Error bars in all graphs are expressed as the mean ± standard error.

## 3. Results

### 3.1. Expression of lysosomal proteins and TFEB increases during the early stages of neuromaturation in cultured neurons

To investigate changes in lysosomes during the early stages of neuronal development, we first analyzed the expression levels of major lysosomal proteins—LAMP1, LIMPII, and Cathepsin D—in rat primary cultured hippocampal neurons at 3, 6, and 9 DIV. The expression levels of all examined lysosomal proteins, both membrane-associated and luminal, were upregulated over time (Fig. 1a–d), suggesting that lysosomal function gradually increases during early neurodevelopment.

These findings suggest that the proteolytic capacity of neuronal lysosomes gradually matures during neurodevelopment and that the metabolic demand for lysosomal activity increases as neurons mature. TFEB is a transcription factor that regulates the expression of most lysosomal genes and controls lysosomal biogenesis and function (Sardiello et al., 2009). Upregulation of TFEB expression directly enhances both lysosomal protein expression and degradative capacity (Sardiello et al., 2009). Notably, TFEB expression was also upregulated across DIV in developing neurons (Fig. 1a and e), suggesting that the expression of lysosomal proteins was at least in part induced by upregulated TFEB levels. We observed that mRNA levels of TFEB shows tendency to elevate with DIV, and the nuclear localization of TFEB protein was significantly increased along with DIV (Supplementary Fig. 1a–c). In addition to overall TFEB expression, its activity is negatively regulated by phosphorylation through mTOR (Vega-Rubin-de-Celis et al., 2017). Downregulation in mTOR activity increases the level of dephosphorylated TFEB, thereby activating lysosome biogenesis. We did not observe detectable levels of phosphorylated TFEB in this study (data not shown). Additionally, the level of phosphorylated S6 ribosomal protein, a reliable indicator of mTOR activity, did not show a significant change during this period (Fig. 1a and f). These findings suggest that the upregulation of lysosomal proteins in early neuronal development is primarily promoted by increased TFEB expression rather than mTOR-mediated regulation of TFEB phosphorylation. In addition to the expression levels of lysosomal proteins, the number of LysoTracker-positive puncta in neurons increased across DIV (Fig. 1g and h), suggesting an increase in lysosome number during neurodevelopment.

### 3.2. Levels of lysosomal proteolysis increase during maturation of cultured neurons

To examine the contribution of lysosomes to intracellular protein degradation during neuromaturation, we performed a pulse-chase assay in developing neurons. We first labeled the total proteins in primary cultured neurons with tritium-labeled leucine for 2 days until 3 DIV. The neurons were then cultured in the presence or absence of specific lysosomal protease inhibitors, pepstatin A and E64d, and the levels of remaining tritium-labeled cellular proteins were measured at 0, 3, and 6 days post-labeling (3, 6, and 9 DIV). The levels of radiolabeled proteins remaining in pepstatin A- and E64d-treated neurons was higher than those in control neurons over DIV (Fig. 2a), suggesting that lysosomal proteolysis was effectively inhibited by the treatment.

To compare total protein degradation levels during early and later stages of neurodevelopment, we next radiolabeled neuronal proteins for 2 days until either 3 or 9 DIV, and measured the radiolabeled protein levels at 0 and 3 days post-labeling to measure the proteolysis levels during these periods (Fig. 2b–d). Protein degradation was significantly lower in pepstatin A- and E64d-treated neurons at both time points (Fig. 2c). Consistent with the increased expression of lysosomal proteins during neuromaturation (Fig. 1a–d), the level of lysosomal proteolysis, inhibited by pepstatin A and E64d, was higher at later DIV than at earlier DIV (Fig. 2d), suggesting that the contribution of lysosomes to cellular proteolysis increases as neurons mature. In contrast, the ratio of lysosomal proteolysis to total protein degradation did not differ significantly between early and late DIV (Fig. 2e). This suggests that the increased lysosomal proteolysis is predominantly proportional to the overall increase in protein degradation demands associated with neuronal growth.

### 3.3. Inhibition of lysosomal proteolysis during the early stages of neuromaturation impairs neuronal morphogenesis and accumulates aggregated protein in the cytoplasm of cultured neurons

Collectively, these data suggest that the requirement for lysosomal activity in developing neurons increases during the early stages of neuromaturation. Therefore, we next examined the effect of impaired lysosomal proteolysis on neuronal development. We transfected primary cultured neurons, maintained in the presence or absence of pepstatin A and E64d, with EGFP to analyze the morphological features of single neurons in each group at 6 DIV. We observed broad disruption in neuronal morphogenesis following treatment with pepstatin A and E64d (Fig. 3a–f). As shown by Sholl analysis (Fig. 3b), both neurite length and complexity decreased under lysosomal proteolysis inhibition. Furthermore, the length of the longest neurite in each cell—presumably the axon—was decreased in pepstatin A- and E64d-treated neurons (Fig. 3c). The standard deviation of the length difference between the longest neurite and other neurites—presumably the dendrites—within the same neuron also decreased under treatment (Fig. 3d), suggesting that the neuronal polarity was impaired. Furthermore, both the number of neurites (Fig. 3e) and the total number of neurite terminals per cell (Fig. 3f) reduced. At an earlier DIV (3 DIV), we observed that the length of Tau1-positive axons was significantly shorter in pepstatin A- and E64d-treated neurons (Fig. 3g and h). In addition, the proportion of neurons exhibiting multiple Tau1-positive protrusions increased in the pepstatin A- and E64d-treated group (Fig. 3g–j). We observed similarly less-polarized localization of Tau1 in pepstatin A- and E64d-treated neurons at 6 DIV (Supplementary Fig. 2a). Collectively, these findings suggest that the establishment of neuronal polarity is disturbed by impaired lysosomal proteolysis during early neurodevelopment. There was no significant change in cytotoxicity with pepstatin A and E64d treatment during this period (Supplementary Fig. 2b).

It has previously been reported that conditional deletion of a gene essential for macroautophagy in adolescent mouse brains results in protein aggregation in mature neurons, accompanied by impaired social behavior resembling ASD (Hui et al., 2019). We speculated that a similar accumulation of aggregated proteins may occur even at earlier stages of development in neurons with impaired lysosomal proteolysis. To test this, we took advantage of Proteostat, a highly sensitive fluorescent dye that directly binds to and visualizes a wide range of aggregated proteins. We observed substantially increased levels of Proteostat-positive signals in the cytoplasm of neurons treated with pepstatin A and E64d at 6 DIV (Fig. 3a and k). This indicates that aggregated proteins accumulate in neurons during early development when lysosomal proteolysis is inhibited.

### 3.4. Ubiquitinated proteins are accumulated in protein aggregates in developing neurons upon inhibition of lysosomal proteolysis

Ubiquitination is an important process for targeting substrate proteins for intracellular degradation via multiple pathways, such as the ubiquitin-proteasome system and selective autophagic pathways (Pohl and Dikic, 2019). Ubiquitinated proteins are also frequently observed as components of protein aggregates in diseases including neurodegenerative disorders and LSDs (Deng et al., 2015; Wilson et al., 2023). We speculated that ubiquitinated proteins may also be components of the aggregated proteins observed in developing neurons with impaired lysosomal proteolysis. To assess this possibility, we first analyzed the total levels of multiubiquitinated proteins in developing neurons and observed a significant increase in neurons cultured with pepstatin A and E64d (Fig. 4a and b). Furthermore, co-immunostaining with Proteostat revealed that the increased multiubiquitinated proteins at least partially colocalizes with aggregated proteins (Fig. 4c and d). Interestingly, a large amount of multiubiquitinated proteins was found surrounding the Proteostat-positive puncta (Fig. 4d). Consistent with this colocalization, we observed that the increased levels of multiubiquitinated proteins were predominantly present in the Triton X-100-insoluble fraction (Fig. 4e). To identify the components of the ubiquitinated proteins in the aggregates, we pulled down the ubiquitinated proteins from the Triton X-100-insoluble fraction (Fig. 4e and f), and subjected them to mass spectrometry analysis. P62 and NBR1, both of which are adaptor proteins for selective degradation of ubiquitinated proteins by

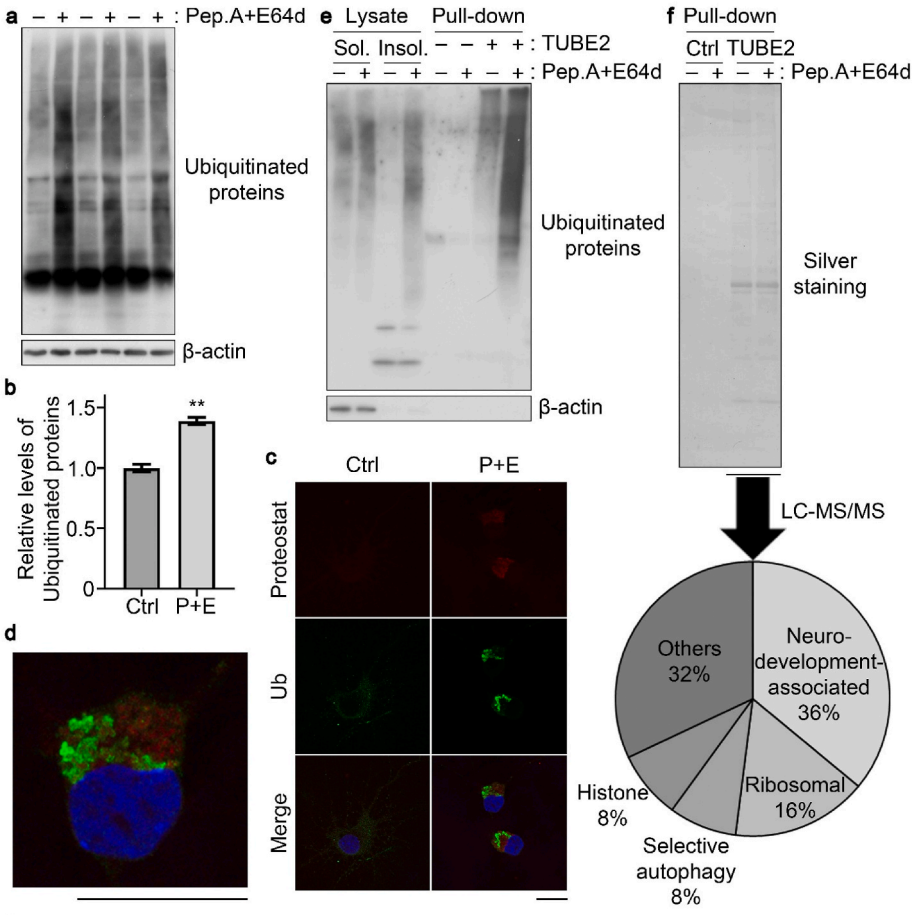


g

| Protein name | Association to neurodevelopment |
|---|---|
| Tubulin beta-3 chain | Neuronal morphology, migration, axon guidance |
| Tubulin beta-5 chain | Neuronal differentialtion, migration, spine formation |
| Myosin light chain 2 | Neuronal morphology, migration, axon guidance, synapse formation |
| Cofilin-1 | Neuronal morphology, migration |
| Kidins220/ARMS | Neuronal morphology |
| EphA4 | Axon guidance, synapse formation, neuronal differentiation |
| DR6/TNFRSF21 | Axon pruning |
| Calcyon | ADHD risk factor |
| DIRAS2 | ADHD risk factor |

**Fig. 4.** Accumulation of ubiquitinated proteins in cultured neurons under lysosomal proteolysis inhibition during neuromaturation (a) Immunoblotting of ubiquitinated proteins in primary cultured hippocampal neurons at 6 DIV, cultured in the absence or presence of pepstatin A and E64d. (b) Quantification of the relative levels of ubiquitinated proteins. (n = 3). (c) Fluorescence microscopy images of primary cultured neurons cultured in the absence or presence of pepstatin A and E64d, co-stained with anti-multiubiquitin chain antibody and Proteostat. (d) An enlarged image of primary neurons cultured in the presence of pepstatin A and E64d, co-stained with anti-multiubiquitin chain antibody and Proteostat. (e) Immunoblotting of ubiquitinated proteins in cell lysates derived from Triton X-100-soluble and -insoluble fractions and pull-down samples derived from Triton X-100-insoluble fractions of primary cultured hippocampal neurons at 6 DIV, cultured in the absence or presence of pepstatin A and E64d. (f) Silver staining of the proteins pulled-down from Triton X-100-insoluble fractions and the summary of Agarose-TUBE2 beads-interacting proteins specifically observed in pepstatin A- and E64d-treated neurons. (g) A list of neurodevelopment-associated proteins interacted with Agarose-TUBE2 beads specifically in pepstatin A- and E64d-treated neurons. Bars represent 20 μm.

macroautophagy and also known as components of pathological protein aggregates, were identified as components specifically in pulled-down sample from pepstatin A- and E64d-treated neurons, confirming the accuracy of the analysis (Supplementary Table 1). In addition, Hsc70 chaperone, a core factor of chaperone-mediated autophagy and also known to localize in protein aggregates, was also identified specifically in pepstatin A- and E64d-treated neuron sample (Supplementary Table 1). Notably, we identified various proteins associated with neuronal development that were specifically present in the pulled-down sample from pepstatin A- and E64d-treated neurons (Fig. 4f and g, Supplementary Table 1) (Higuero et al., 2010; Javier-Torrent and Saura, 2020; Laurin et al., 2005; Ohashi, 2015; Olsen et al., 2014; Reif et al., 2011; Tantry and Santhakumar, 2023; Verma et al., 2023). Together, these results suggests that multiubiquitinated protein aggregates can accumulate from the early stages of neuronal development and may interrupt normal neuromaturation by sequestering proteins critical for neuronal development.

### 3.5. *Inhibition of lysosomal proteolysis during neuromaturation impairs the acquisition of neuronal identity in cultured neurons*

Lastly, we sought to examine how the accumulation of aggregated proteins caused by defective lysosomal proteolysis could contribute to impaired morphogenesis in developing neurons. Previous studies have

reported that Huntington's disease, a prototypical neurodegenerative disorder, involves neurodevelopmental abnormalities (Barnat et al., 2020; Conforti et al., 2018). The expression of mutant huntingtin, an aggregative protein, has been shown to disrupt the acquisition of neuronal identity and impair the maturation and differentiation of neuronal cells (Conforti et al., 2018). In such circumstances, the expression of various proteins associated with neuromaturation is decreased or abolished. Similarly, impaired neuronal maturation and morphogenesis due to defective macroautophagy during adult neurogenesis have also been documented (Schaffner et al., 2018). To examine the impact of defective lysosomal proteolysis on neuromaturation, we analyzed the expression levels of several neuronal lineage marker proteins whose expression correlates with neuronal maturation. In control neurons, the expression of all three markers examined—β3-tubulin, a marker of immature postmitotic neurons; Fox-3, and MAP2, both markers of mature neurons—increased over time by 9 DIV (Fig. 5a–d). However, the expression levels of all three proteins failed to increase significantly and instead declined by 9 DIV in pepstatin A- and E64d-treated neurons (Fig. 5a–d). Together with the widespread morphological disruptions (Fig. 3a–k) and the sequestration of neurodevelopment-associated proteins into ubiquitinated protein aggregates (Fig. 4f and g), these findings suggest that acquisition of neuronal identity is impaired in developing neurons under disrupted lysosomal proteolysis. Importantly, we observed similar impairment in morphogenesis, accumulation of ubiquitinated protein aggregates in the Triton X-100-insoluble fraction, and the decline in expression levels of neuronal lineage marker proteins in neurons cultured in the presence of ammonium chloride to inhibit lysosomal hydrolases (Supplementary Fig. 3 a–f). The fact inhibiting lysosomal degradative capacity with different procedures results in analogous consequences further supports that impaired lysosomal proteolysis in developing neurons induces protein aggregation and disrupts morphogenesis and neuromaturation.

## 4. Discussion

In this study, we observed a time-dependent increase in the requirement for, and contribution of, lysosomal proteolytic capacity during the early stages of neuronal development *in vitro*. Impaired lysosomal proteolysis disrupted neuromaturation and led to the intracellular accumulation of aggregated proteins. The upregulation of

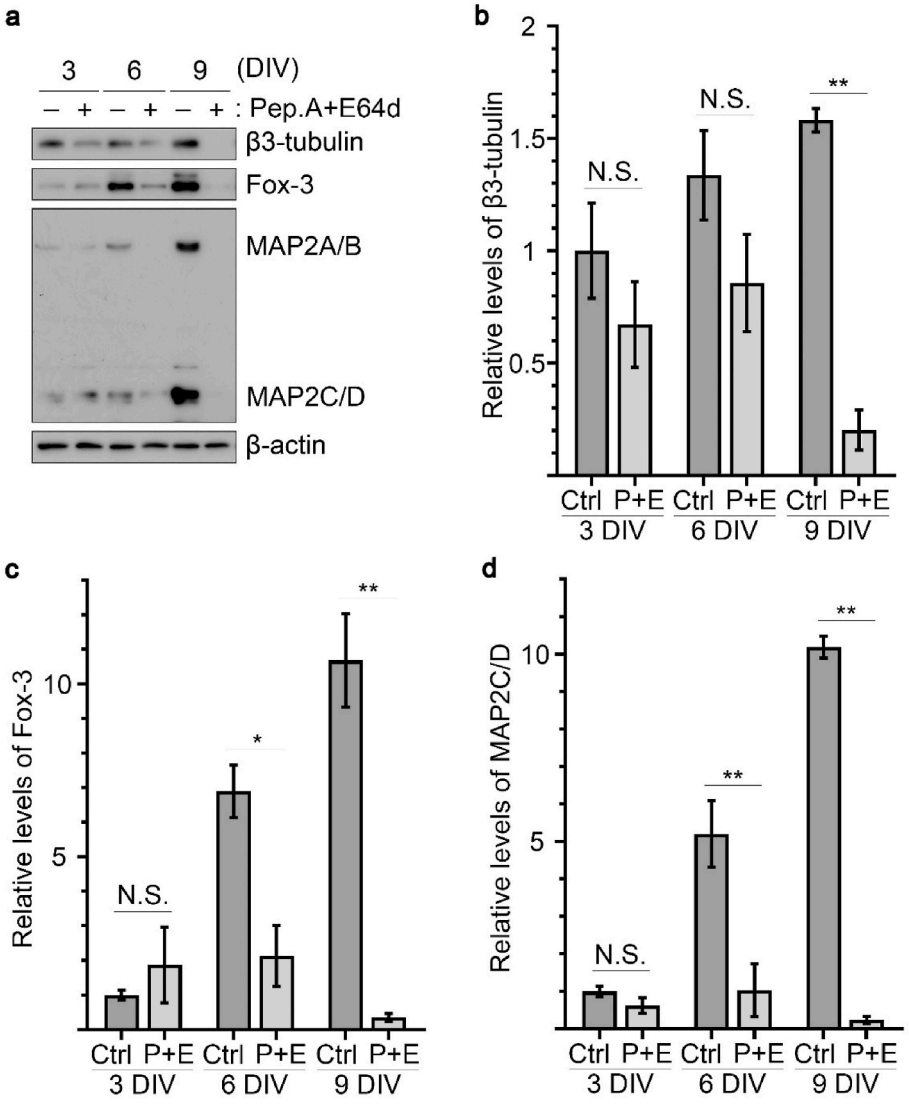


**Fig. 5.** Expression levels of neuronal lineage marker proteins in cultured neurons under lysosomal proteolysis inhibition at the early stages of neuromaturation (a) Expression levels of β3-tubulin, Fox-3, and MAP2 in primary cultured hippocampal neurons cultured in the presence or absence of pepstatin A and E64d. (b–d) Quantification of the relative levels of β3-tubulin (b), Fox-3 (c), and MAP2C/D (d) in primary cultured hippocampal neurons cultured in the presence or absence of pepstatin A and E64d. (n = 3). *$p < 0.05$, **$p < 0.01$; N.S., not significant. P + E, pepstatin A and E64d.

lysosomal proteins during neurodevelopment appeared to result from increased expression of TFEB, rather than from mTOR-mediated changes in TFEB phosphorylation (Fig. 1a–f). Given that mTOR oppositely regulates the synthesis and degradation of cellular components (Napolitano et al., 2022), mTOR-independent lysosomal upregulation may be reasonable in developing neurons, where both anabolic and catabolic processes are critical. The accumulation of aggregated proteins has previously been reported in mature neurons of adolescent mice exhibiting ASD-like behaviors associated with impaired macroautophagy (Hui et al., 2019), as well as in patients and animal models of various LSDs and neurodegenerative diseases (Ballabio and Bonifacino, 2020; Navarro-Romero et al., 2020; Nixon, 2013; Platt et al., 2018). However, the protein aggregates observed in our study formed in neurons at earlier developmental stages—during axonal and dendritic outgrowth (Banker, 2018; Dotti et al., 1988). These findings suggest that protein aggregation due to disrupted cellular metabolic balance, and its impact on neuronal homeostasis and function, can occur much earlier than we may have expected. Because the Proteostat dye is approximately two orders of magnitude more sensitive to aggregated proteins than conventional dyes such as Thioflavin T (Shen et al., 2011), the existence of aggregated proteins in neurons in their early development may have been left untouched.

In this study, we also observed a significant decline in the overall expression levels of neuronal lineage marker proteins in developing neurons following impaired lysosomal proteolytic capacity (Fig. 5a–d). The reduction in Fox-3 and MAP2, mature neuron markers, was more severe than that of β3-tubulin, an immature postmitotic neuron marker (Fig. 5a–d). Notably, among MAP2 isoforms, MAP2C/D is typically expressed during early developmental stages, whereas MAP2A/B levels increase subsequently along with maturation (Jalava et al., 2007). The expression of MAP2A/B appeared to be more severely affected by defects in lysosomal proteolysis, compared with that of MAP2C/D (Fig. 5a), further suggesting that the decline in the levels of these neuronal proteins is associated with impairment in neuromaturation. Although the mechanisms underlying this reduction in neuronal lineage marker proteins remain to be elucidated, it is noteworthy that various proteins associated with development of neurons, including β3-tubulin, was identified among the ubiquitinated protein aggregates specifically present in pepstatin A- and E64d-treated neurons (Fig. 4g). The sequestration of neurodevelopment-associated proteins into protein aggregates may be one of the upstream events contributing to impaired neuromaturation. However, it should be noted that the gel-based proteomics analysis used in this study has limited sensitivity, and numerous yet unidentified proteins may be present within the aggregates. In aggregative proteins observed in both neurodegenerative diseases and LSDs, similarities in their components such as phosphorylated tau and α-synuclein have been reported in previous studies (Ballabio and Bonifacino, 2020; Navarro-Romero et al., 2020). Furthermore, expression of mutant huntingtin, an aggregative protein has been reported to disturb neuromaturation (Conforti et al., 2018). We did not detect the causative gene products of known neurodegenerative disorders among the protein aggregates in this study; however, the accumulation of aggregated proteins in neurons may represent a shared pathophysiological aspect linking neurodegenerative diseases, LSDs, and neurodevelopmental disorders, associated with impaired lysosomal degradation pathways. In this study, we did not examine further into the specific autophagic pathways responsible for lysosomal proteolysis during early neurodevelopment. Involvement of upstream pathways, including autophagic pathways other than macroautophagy, such as microautophagy and chaperone-mediated autophagy, in neurodevelopment also warrants further investigation.

## CRediT authorship contribution statement

**Yinping Zhou:** Writing – review & editing, Writing – original draft, Visualization, Investigation, Formal analysis, Data curation. **Yuuki Fujiwara:** Writing – review & editing, Writing – original draft, Visualization, Supervision, Project administration, Methodology, Investigation, Funding acquisition, Data curation, Conceptualization. **Mai Shirazaki:** Validation, Investigation. **Xiaoye Tian:** Investigation. **Gen Igarashi:** Validation. **Hiroto Yamauchi:** Validation. **Kazunori Imaizumi:** Funding acquisition, Writing – review & editing. **Hideki Hayakawa:** Writing – review & editing. **Ko Miyoshi:** Writing – review & editing. **Taiichi Katayama:** Writing – review & editing, Supervision.

## Funding

This work was supported by Grants-in-Aid for Scientific Research from the Japan Society for the Promotion of Science (21K15367 and 23K14453 to Y.F. and 23K17413 to K.I.), ACT-X from the Japan Science and Technology Agency (JPMJAX222H to Y.F.), Research Grant for Medical Research from the Osaka Medical Research Foundation for Intractable Diseases (to Y.F.), and Grant Program for Research Study from the Nakatani Foundation for Advancement of Measuring Technologies in Biomedical Engineering (to Y.F.).

## Declaration of competing interest

None.

## Acknowledgements

We thank Umihito Nakagawa and Ayako Nishioka of CoMIT Omics Center, Graduate School of Medicine, Osaka University for technical support, and Editage for English language editing.

## Appendix A. Supplementary data

Supplementary data to this article can be found online at https://doi.org/10.1016/j.neuint.2025.106048.

## Data availability

The data generated or analyzed in this study are available from the corresponding author on reasonable request.

## References

Appelqvist, H., Waster, P., Kagedal, K., Ollinger, K., 2013. The lysosome: from waste bag to potential therapeutic target. J. Mol. Cell Biol. 5, 214–226.
Ballabio, A., Bonifacino, J.S., 2020. Lysosomes as dynamic regulators of cell and organismal homeostasis. Nat. Rev. Mol. Cell Biol. 21, 101–118.
Banker, G., 2018. The development of neuronal polarity: a retrospective view. J. Neurosci. 38, 1867–1873.
Barnat, M., Capizzi, M., Aparicio, E., Boluda, S., Wennagel, D., Kacher, R., Kassem, R., Lenoir, S., Agasse, F., Braz, B.Y., Liu, J.P., Ighil, J., Tessier, A., Zeitlin, S.O., Duyckaerts, C., Dommergues, M., Durr, A., Humbert, S., 2020. Huntington's disease alters human neurodevelopment. Science 369, 787–793.
Battaglioni, S., Benjamin, D., Walchli, M., Maier, T., Hall, M.N., 2022. mTOR substrate phosphorylation in growth control. Cell 185, 1814–1836.
Collier, J.J., Guissart, C., Olahova, M., Sasorith, S., Piron-Prunier, F., Suomi, F., Zhang, D., Martinez-Lopez, N., Leboucq, N., Bahr, A., Azzarello-Burri, S., Reich, S., Schols, L., Polvikoski, T.M., Meyer, P., Larrieu, L., Schaefer, A.M., Alsaif, H.S., Alyamani, S., Zuchner, S., Barbosa, I.A., Deshpande, C., Pyle, A., Rauch, A., Synofzik, M., Alkuraya, F.S., Rivier, F., Ryten, M., McFarland, R., Delahodde, A., McWilliams, T.G., Koenig, M., Taylor, R.W., 2021. Developmental consequences of defective ATG7-Mediated autophagy in humans. N. Engl. J. Med. 384, 2406–2417.
Conforti, P., Besusso, D., Bocchi, V.D., Faedo, A., Cesana, E., Rossetti, G., Ranzani, V., Svendsen, C.N., Thompson, L.M., Toselli, M., Biella, G., Pagani, M., Cattaneo, E., 2018. Faulty neuronal determination and cell polarization are reverted by modulating HD early phenotypes. Proc. Natl. Acad. Sci. U. S. A. 115, E762–E771.
de Duve, C., Pressman, B.C., Gianetto, R., Wattiaux, R., Appelmans, F., 1955. Tissue fractionation studies. 6. Intracellular distribution patterns of enzymes in rat-liver tissue. Biochem. J. 60, 604–617.
Deng, H., Xiu, X., Jankovic, J., 2015. Genetic convergence of Parkinson's disease and lysosomal storage disorders. Mol. Neurobiol. 51, 1554–1568.
Dotti, C.G., Sullivan, C.A., Banker, G.A., 1988. The establishment of polarity by hippocampal neurons in culture. J. Neurosci. 8, 1454–1468.

Higuero, A.M., Sanchez-Ruiloba, L., Doglio, L.E., Portillo, F., Abad-Rodriguez, J., Dotti, C.G., Iglesias, T., 2010. Kidins220/ARMS modulates the activity of microtubule-regulating proteins and controls neuronal polarity and development. J. Biol. Chem. 285, 1343–1357.
Hui, K.K., Takashima, N., Watanabe, A., Chater, T.E., Matsukawa, H., Nekooki-Machida, Y., Nilsson, P., Endo, R., Goda, Y., Saido, T.C., Yoshikawa, T., Tanaka, M., 2019. GABARAPs dysfunction by autophagy deficiency in adolescent brain impairs GABA(A) receptor trafficking and social behavior. Sci. Adv. 5, eaau8237.
Jalava, N.S., Lopez-Picon, F.R., Kukko-Lukjanov, T.K., Holopainen, I.E., 2007. Changes in microtubule-associated protein-2 (MAP2) expression during development and after status epilepticus in the immature rat hippocampus. Int. J. Dev. Neurosci. 25, 121–131.
Javier-Torrent, M., Saura, C.A., 2020. Conventional and non-conventional roles of non-muscle Myosin II-Actin in neuronal development and degeneration. Cells 9.
Laurin, N., Misener, V.L., Crosbie, J., Ickowicz, A., Pathare, T., Roberts, W., Malone, M., Tannock, R., Schachar, R., Kennedy, J.L., Barr, C.L., 2005. Association of the calcyon gene (DRD1IP) with attention deficit/hyperactivity disorder. Mol. Psychiatr. 10, 1117–1125.
Linda, K., Lewerissa, E.I., Verboven, A.H.A., Gabriele, M., Frega, M., Klein Gunnewiek, T. M., Devilee, L., Ulferts, E., Hommersom, M., Oudakker, A., Schoenmaker, C., van Bokhoven, H., Schubert, D., Testa, G., Koolen, D.A., de Vries, B.B.A., Nadif Kasri, N., 2022. Imbalanced autophagy causes synaptic deficits in a human model for neurodevelopmental disorders. Autophagy 18, 423–442.
Lo, L.H., Lai, K.O., 2020. Dysregulation of protein synthesis and dendritic spine morphogenesis in ASD: studies in human pluripotent stem cells. Mol. Autism 11, 40.
Napolitano, G., Di Malta, C., Ballabio, A., 2022. Non-canonical mTORC1 signaling at the lysosome. Trends Cell Biol. 32, 920–931.
Navarro-Romero, A., Montpeyo, M., Martinez-Vicente, M., 2020. The emerging role of the lysosome in Parkinson's Disease. Cells 9.
Nixon, R.A., 2013. The role of autophagy in neurodegenerative disease. Nat. Med. 19, 983–997.
Nixon, R.A., Rubinsztein, D.C., 2024. Mechanisms of autophagy-lysosome dysfunction in neurodegenerative diseases. Nat. Rev. Mol. Cell Biol. 25, 926–946.
Ohashi, K., 2015. Roles of cofilin in development and its mechanisms of regulation. Dev. Growth Differ. 57, 275–290.
Olsen, O., Kallop, D.Y., McLaughlin, T., Huntwork-Rodriguez, S., Wu, Z., Duggan, C.D., Simon, D.J., Lu, Y., Easley-Neal, C., Takeda, K., Hass, P.E., Jaworski, A., O'Leary, D. D., Weimer, R.M., Tessier-Lavigne, M., 2014. Genetic analysis reveals that amyloid precursor protein and death receptor 6 function in the same pathway to control axonal pruning independent of beta-secretase. J. Neurosci. 34, 6438–6447.
Parenti, I., Rabaneda, L.G., Schoen, H., Novarino, G., 2020. Neurodevelopmental disorders: from genetics to functional pathways. Trends Neurosci. 43, 608–621.
Platt, F.M., d'Azzo, A., Davidson, B.L., Neufeld, E.F., Tifft, C.J., 2018. Lysosomal storage diseases. Nat. Rev. Dis. Primers 4, 27.
Pohl, C., Dikic, I., 2019. Cellular quality control by the ubiquitin-proteasome system and autophagy. Science 366, 818–822.
Reif, A., Nguyen, T.T., Weissflog, L., Jacob, C.P., Romanos, M., Renner, T.J., Buttenschon, H.N., Kittel-Schneider, S., Gessner, A., Weber, H., Neuner, M., Gross-Lesch, S., Zamzow, K., Kreiker, S., Walitza, S., Meyer, J., Freitag, C.M., Bosch, R., Casas, M., Gomez, N., Ribases, M., Bayes, M., Buitelaar, J.K., Kiemeney, L.A., Kooij, J.J., Kan, C.C., Hoogman, M., Johansson, S., Jacobsen, K.K., Knappskog, P.M., Fasmer, O.B., Asherson, P., Warnke, A., Grabe, H.J., Mahler, J., Teumer, A., Volzke, H., Mors, O.N., Schafer, H., Ramos-Quiroga, J.A., Cormand, B., Haavik, J., Franke, B., Lesch, K.P., 2011. DIRAS2 is associated with adult ADHD, related traits, and co-morbid disorders. Neuropsychopharmacology 36, 2318–2327.
Sardiello, M., Palmieri, M., di Ronza, A., Medina, D.L., Valenza, M., Gennarino, V.A., Di Malta, C., Donaudy, F., Embrione, V., Polishchuk, R.S., Banfi, S., Parenti, G., Cattaneo, E., Ballabio, A., 2009. A gene network regulating lysosomal biogenesis and function. Science 325, 473–477.
Schaffner, I., Minakaki, G., Khan, M.A., Balta, E.A., Schlotzer-Schrehardt, U., Schwarz, T. J., Beckervordersandforth, R., Winner, B., Webb, A.E., DePinho, R.A., Paik, J., Wurst, W., Klucken, J., Lie, D.C., 2018. FoxO function is essential for maintenance of Autophagic Flux and neuronal morphogenesis in adult neurogenesis. Neuron 99, 1188–1203 e1186.
Shen, D., Coleman, J., Chan, E., Nicholson, T.P., Dai, L., Sheppard, P.W., Patton, W.F., 2011. Novel cell- and tissue-based assays for detecting misfolded and aggregated protein accumulation within aggresomes and inclusion bodies. Cell Biochem. Biophys. 60, 173–185.
Tanida, I., Minematsu-Ikeguchi, N., Ueno, T., Kominami, E., 2005. Lysosomal turnover, but not a cellular level, of endogenous LC3 is a marker for autophagy. Autophagy 1, 84–91.
Tantry, M.S.A., Santhakumar, K., 2023. Insights on the role of alpha- and beta-Tubulin isotypes in early brain development. Mol. Neurobiol. 60, 3803–3823.
Vega-Rubin-de-Celis, S., Pena-Llopis, S., Konda, M., Brugarolas, J., 2017. Multistep regulation of TFEB by MTORC1. Autophagy 13, 464–472.
Verma, M., Chopra, M., Kumar, H., 2023. Unraveling the potential of EphA4: a breakthrough target and beacon of hope for neurological diseases. Cell. Mol. Neurobiol. 43, 3375–3391.
Wilson 3rd, D.M., Cookson, M.R., Van Den Bosch, L., Zetterberg, H., Holtzman, D.M., Dewachter, I., 2023. Hallmarks of neurodegenerative diseases. Cell 186, 693–714.
Yim, W.W., Mizushima, N., 2020. Lysosome biology in autophagy. Cell. Discov. 6, 6.